Supplementary information for:

COVID-19 diagnosis and SARS-CoV-2 strain identification by a rapid, multiplexed, point-of-care antibody microarray

Authors: Jacob T. Heggestad,[1†] Rhett J. Britton,[1†] David S. Kinnamon,[1†] Jason Liu,[1] Jack G. Anderson,[2] Daniel Y. Joh,[1] Zachary Quinn,[1] Cassio M. Fontes,[1] Angus M. Hucknall,[1] Robert Parks,[3] Gregory D. Sempowski,[3,4] Thomas N. Denny,[3] Thomas W. Burke,[3] Barton F. Haynes,[3,4,5] Christopher W. Woods,[2,3,4] Ashutosh Chilkoti[1*]

Affiliations:

[1] Department of Biomedical Engineering, Pratt School of Engineering, Duke University, Durham, NC 27708, USA.

[2] Center for Applied Genomics and Precision Medicine, Department of Medicine, Duke University, Durham, NC 27710, USA.

[3] Duke Human Vaccine Institute, Duke University School of Medicine, Durham, NC 27710, USA.

[4] Department of Medicine, Duke University School of Medicine, Durham, NC 27710, USA.

[5] Department of Immunology, Duke University School of Medicine, Durham, NC, USA

*To whom correspondence should be addressed: Ashutosh Chilkoti (chilkoti@duke.edu).
[†]These authors contributed equally to this work.

Contents

Experimental methods

CoVariant-SPOT fabrication

CoVariant-SPOT employs the technology of the D4 assay, described previously.[1] In brief, glass microscope slides were functionalized with a poly(oligo(ethylene glycol) methyl ether methacrylate (POEGMA) non-fouling brush with a thickness of ~50 nm via surface-initiated atom transfer radical polymerization (SI-ATRP).[2] Next, anti-SARS-CoV-2 N protein monoclonal antibody (mouse IgG, DHVI, 1B2) and anti-SARS-CoV-2 S protein monoclonal antibodies (Acro Biosystems, catalog #S1N-M130; Sino Biological, catalog #40591-MM43; Sino Biological, catalog #40591-MM48) were inkjet printed onto the slides using a Scienion sciFLEXARRAYER S12 (Scienion AG). Rows of five ~180 µm diameter capture spots for each anti-SARS-CoV-2 antibody were printed at a concentration of 1.0 mg/mL. Surrounding the capture spots, twelve 1 mm-diameter trehalose spots were printed using a BioDot AD1520 printer (BioDot Inc.) loaded with a 10% (w/v) trehalose solution (~100 nL drop volume). Next, Alexa Fluor 647 labeled anti-N antibody (human IgG, DHVI, DH1218) and anti-S antibody (Acro Biosystems, catalog # S1N-M122) were mixed and deposited on top of the excipient pads using the BioDot printer at a concentration of 0.02 mg/mL for each antibody. Twenty-four assays with this configuration were printed on each 75.6 x 25.0 x 1.0 mm glass slide in a 3 x 8 array. CoVariant-SPOT assays were stored under vacuum for at least 24 h before use. For testing with clinical samples, Trublock Ultra (Meridian Life Sciences) was also inkjet printed onto CoVariant-SPOT slides at 6.0 mg/mL in 1x PBS with 0.05% sodium azide in order to prevent any potential interference from human anti-mouse antibodies (HAMA), as described elsewhere.[3]

To identify antibodies for CoVariant-SPOT, we conducted high throughput screens to determine optimal cAb/dAb pairs that bound to SARS-CoV-2 variants differentially. For antibodies targeting S protein, we screened 29 potential cAbs and 13 potential dAbs against WT, Delta, and Omicron S1 proteins, resulting in 1131 different dose-response curves. We also screened the antibodies against Beta S1, leading to a total of 1508 dose-response curves (Figure S1). All antibodies tested are listed in **Table S2**. In this screening process, all 29 candidate cAbs are inkjet printed onto POEGMA coated slides in a microarray. Next, recombinant S1 proteins for each variant are individually spiked into fetal bovine serum at multiple concentrations and added to the arrays containing all 29 cAbs. After a 30-minute incubation, slides are washed, and then a dAb is added to complete the sandwich formation process, resulting in 29 dose-response curves per dAb per S1 protein. After repeating this process for each dAb and S1 protein variant, we identified three potential cAbs for S1 (for a given dAb) that could potentially be used to differentiate between WT, Delta, and Omicron, depending on the fluorescence output at each cAb spot. The anti-S1 antibody pairs we identified also bind to the S trimers for WT, Delta, and Omicron variants similarly compared to S1 (Figure S2). For detection of N, we incorporated an antibody pair identified by the Duke Human Vaccine Institute (DHVI). Therefore, the final version of the CoVariant-SPOT featured four cAbs (three targeting S protein and one targeting N protein) and a dAb cocktail consisting of one dAb targeting S protein and one dAb targeting N protein. Of note, we can perform these high throughput antibody screens rapidly—on the order of a couple of days—which enables us to rapidly incorporate more antibodies into CoVariant-SPOT if new variants emerge or to better discriminate between variants.

Viral RNA Extraction and Sequencing Library Preparation

Viral RNA was extracted from nasopharyngeal swabs in VTM using QIAamp Viral RNA Mini Kit (QIAGEN). Sequencing libraries were prepared using the Illumina COVIDSeq Test SARS-CoV-2 kit at a reduced quarter volume reaction on liquid handlers. Libraries were pooled at equal volume, and the pool's concentration and library size were quantified with the Invitrogen Qubit 4 Fluorometer and Agilent Tapestation. The final pool was sequenced on the Illumina NextSeq500 instrument using a 75 cycle High Output flow cell with 72 base pair single reads, 1.5pM loading concentration, and 5% PhiX v3 control spike-in.

Variant Analysis Pipeline

To classify COVID-19 variants, it is necessary to identify the mutations along each genome. To do this, we used a custom analytical pipeline based on the best practices workflow from GATK.[4] The custom scripts and tools

with instructions for installation and execution of the pipeline are not currently available for public access but will be shared upon request. Briefly, our analysis starts with trimming Nextera adapters from each sequence, then individual reads with low quality scores (<q20) are eliminated. Next, the trimmed reads are aligned to the SARS-CoV-2 reference genome using BWA.[5] In this study, we used the isolate Wuhan-Hu-1 obtained from GenBank (Accession Number: NC_045512.2). Next, our customized GATK Workflow[4] is automatically run to identify single nucleotide polymorphisms (SNPs), insertions and deletions (INDELS) along the 29 kb of the SARS-CoV-2 genome. We used one pass of base quality score recalibration to generate high quality SNPs and INDELS, an important step for correcting errors produced during the alignment process and improves accuracy of variant calls. Next, a package called HaplotypeCaller was used to identify variants assuming a ploidy of "1". Generating a VCF file that undergoes hard filtering using the VariantFiltration command, and a summary statistics table that allows assessing the quality of each of the resulting genotypes. Finally, the VCF tables are used to generate consensus genomes in FASTA format using BCFtools v1.15.1.[6] Next, each genome is concatenated into a larger file and processed with Pangolin v.4.1.2 to identify and classify the variant identity of each genome.[7]

Quantitative RT-PCR

Method 1: SARS-CoV-2 PCR viral load – nasopharyngeal swab: Nasal swab VTM was aliquoted and cryopreserved from study subjects to determine SARS-CoV-2 N1 gene copy number by RT-PCR to stratify subjects as COVID PCR positive or negative. Viral RNA was extracted from 140 µL of VTM according to manufacturer's instructions (QiaAmp Viral RNA minikit). SARS-CoV-2 nucleocapsid (N1) and human RNase P (RPP30) RNA copies were determined using 5 µL of isolated RNA in the CDC-designed kit (CDC-006-00019, Revision: 03, Integrated DNA Technologies 2019-nCoV kit). Standard quantitative RT-PCR (TaqPath 1-step RT qPCR Master Mix, Thermofisher) was run with NP1 RNA standard (Integrated DNA Technologies) and gene-specific standard curves (2e5 copy/mL – 20 copy/mL). Regression analysis was used to determine NP1 gene copy number and corrected to report copies/mL of VTM. Samples with a Ct value >35 are called as COVID PCR NEGATIVE and samples ≤35 are called COVID PCR POSITIVE.

Method 2: SARS-CoV-2 "High Sensitivity" qPCR viral load: Lab Developed Test (LDT) qPCR for SARS-CoV-2 Total RNA E-gene (envelope). Method: QIAGEN QIAsymphony DSP Virus/Pathogen Midi Kit (96)/QIAgility was used for isolation and purification of nucleic acids. PCR was run on Applied Biosystems QuantStudio 3 Real-Time PCR System. For each batch, a standard curve was run to extrapolate RNA copies/mL. NP/VTM (0.5ml) was diluted 1:1 with PBS and 0.8 mL input for RNA extractions (0.4 mL equivalent VTM). Assays were run in singlicate. Any positive VL detected is considered "Positive". Not detected is considered "Negative". The lower limit of quantification (LLOQ) for this assay was 128 RNA cp/mL for 0.4ml 1:1 diluted input. Values below the LOQ may be outside of the 95% confidence interval for reproducibility.

Microfluidic CoVariant-SPOT

The cassette is based on designs previously published.[8] To perform a test, ~72 µL of sample is added by dropper to the sample inlet, followed by addition of wash buffer to the second well. All assay reagents are inkjet printed within the reaction chamber. After sample addition, the four steps of the D4 assay take place in the reaction chamber, resulting in the formation of antibody sandwiches with the analyte. Simultaneously, a small volume of sample traverses the snaking timing channels, which govern the incubation time. Once the sample reaches the outlet of the timing channel, the sample is absorbed into a wicking pad that is situated at the outlet of the timing channel. This removes sample and unbound reagent from the reaction chamber, while also flushing the chamber with wash buffer. Once the wash buffer is also absorbed, a clean and dry surface is ready for imaging on the D4Scope.

The cassettes were fabricated using a laser ablation manufacturing process. Complementary layers of patterned acrylic (1mm Clarex, Astra Products) and double-sided adhesive (9474LE, 3M company) were fabricated using an LS900 Gravograph CO_2 laser cutter (Gravotech, Inc.) based on template files created in AutoCAD 2022 (Autodesk, Inc.). Layers were precisely assembled using a custom designed 3D-printed alignment device

(**Figure S9**). Final assembly included affixing the sample inlet and wash buffer reservoir to the top of the cassette and adding the wicking pads to the outlet of the timing channel (Whatman CF7 100% cotton liner). The inlet reservoir and alignment device were designed in Solidworks 2019 and 3D printed using a Form 3 SLA printer (Form Labs, Inc.).

The cassette features an upper and a lower section of its reaction chamber with the same CoVariant-SPOT reagents as described before. Alexa Fluor 647 labeled anti-N antibody and anti-S antibody were mixed and deposited in the upper reaction chamber as three 100 nL spots at a concentration of 0.10 mg/mL for each antibody in 10% (w/v) trehalose 1x PBS. To aid in dissolution during testing, the detection antibodies were printed on top of three 10% (w/v) trehalose excipient pads in 1x PBS. In the lower chamber, one anti-N and three anti-S antibodies were inject printed in spatially distinct 360 pL spots diluted in 0.05% (w/v) trehalose in 1x PBS. To normalize for any gradient effect in the reaction chamber or for uneven excitation of the D4Scope laser, the four printed cAbs were randomly addressed in the reaction chamber (**Figure 5A**). Additionally, four fiducial spots of anti-Cy5 antibody (Millipore Sigma, catalog number: C1117) at 0.33 mg/mL were printed adjacent to the cAbs. These spots were used for D4Scope alignment and as an assay control.

An objective outlier removal algorithm was used on the resulting calculated fluorescence intensities using Microsoft Excel. First, a minimum fluorescence threshold of 100 a.u. was assigned to any spot that fell below the threshold after background subtraction. Next, outliers were removed using two passes of a 1.5 times interquartile range removal criteria. If greater than 50% of capture spots for a single cAb on a cassette were flagged as outliers, they would be removed from analysis (this did not occur in this study).

D4Scope

The D4Scope is composed of a Basler Ace CMOS Camera module (AcA3088-57um, Basler AG), 676/37-25 nm bandpass filter (Semrock), MC100X lens (Optoengineering), and an obliquely angled (30°) 638nm red laser module (Sharp). Mounts and housings for the optical components and holder for the microfluidic cassette holder were 3D printed via selective laser sintering with a Formlabs Fuse 1 (Formlabs Inc.). The D4Scope can be controlled either from a built-in Raspberry Pi 4B 2GB (Raspberry Pi Foundation) with accompanying 3.5” TFT LCD display (UCTRONCIS) or directly from a personal computer via a USB 3.0 connection.

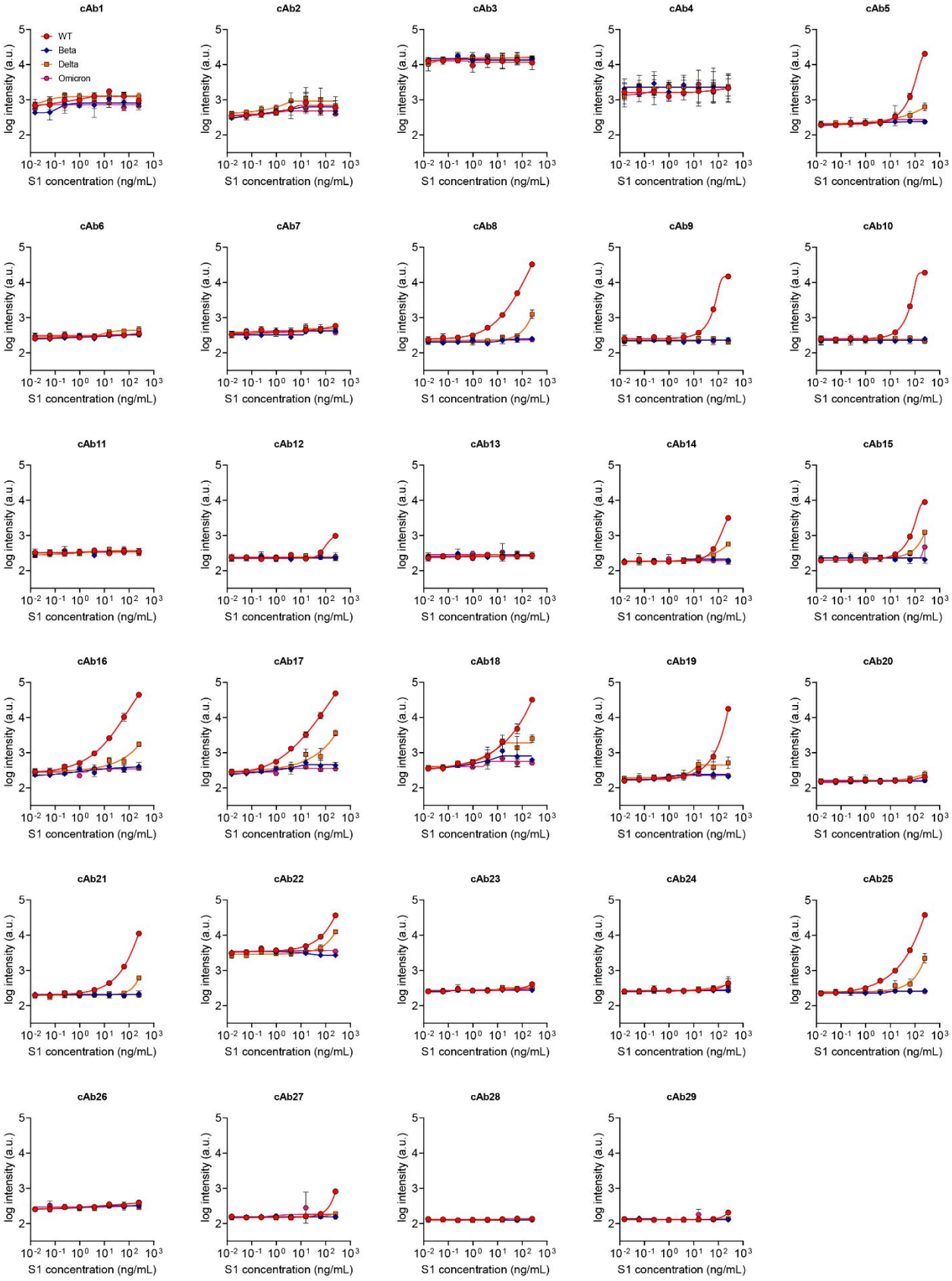
dAb4
cAb1
cAb2
cAb3
cAb4
cAb5
cAb6
cAb7
cAb8
cAb9
cAb10
cAb11
cAb12
cAb13
cAb14
cAb15
cAb16
cAb17
cAb18
cAb19
cAb20
cAb21
cAb22
cAb23
cAb24
cAb25
cAb26
cAb27
cAb28
cAb29
WT
Beta
Delta
Omicron
log intensity (a.u.)
S1 concentration (ng/mL)

dAb5

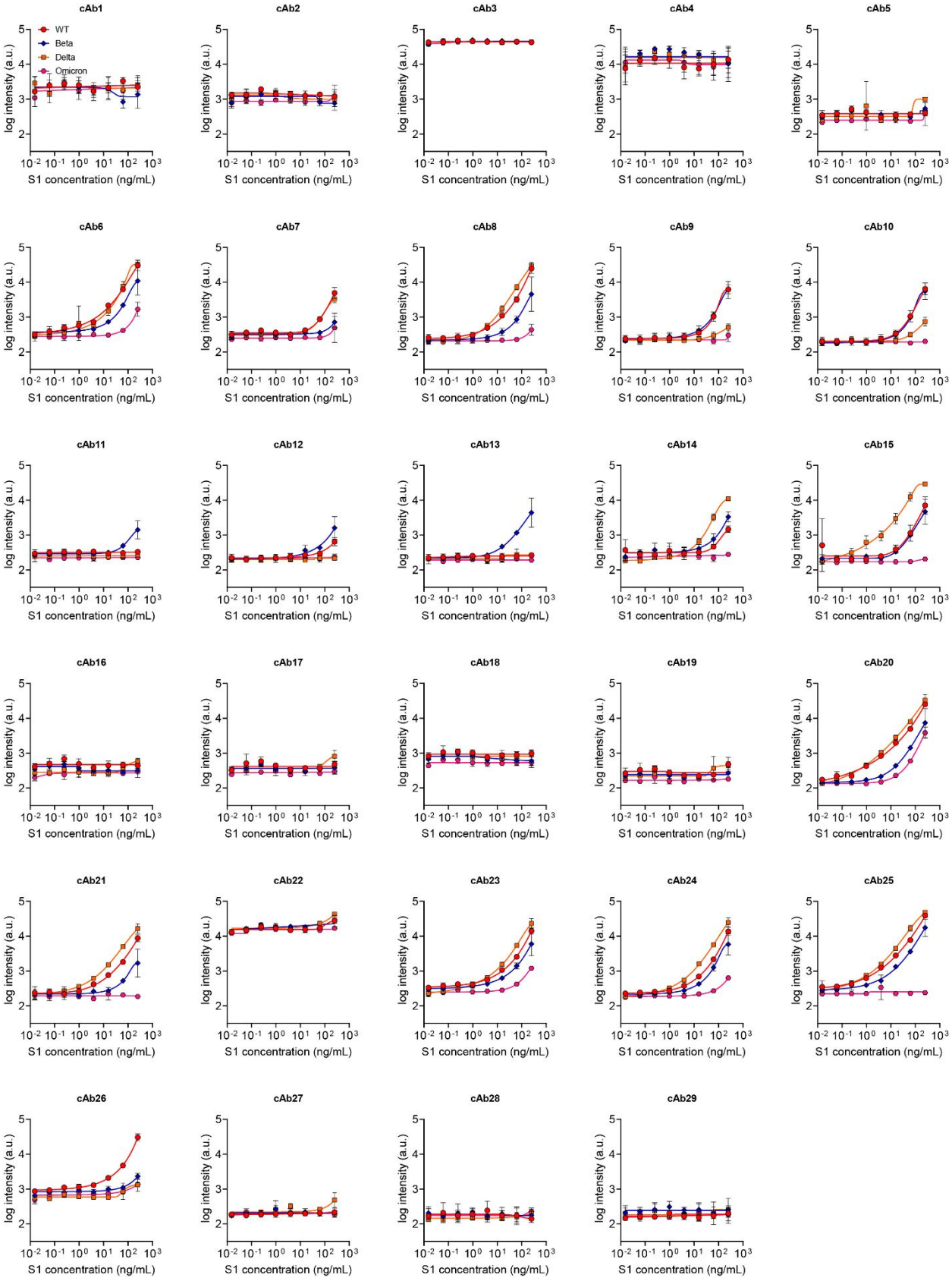
cAb1
cAb2
cAb3
cAb4
cAb5
cAb6
cAb7
cAb8
cAb9
cAb10
cAb11
cAb12
cAb13
cAb14
cAb15
cAb16
cAb17
cAb18
cAb19
cAb20
cAb21
cAb22
cAb23
cAb24
cAb25
cAb26
cAb27
cAb28
cAb29
WT
Beta
Delta
Omicron
log intensity (a.u.)
S1 concentration (ng/mL)

dAb6

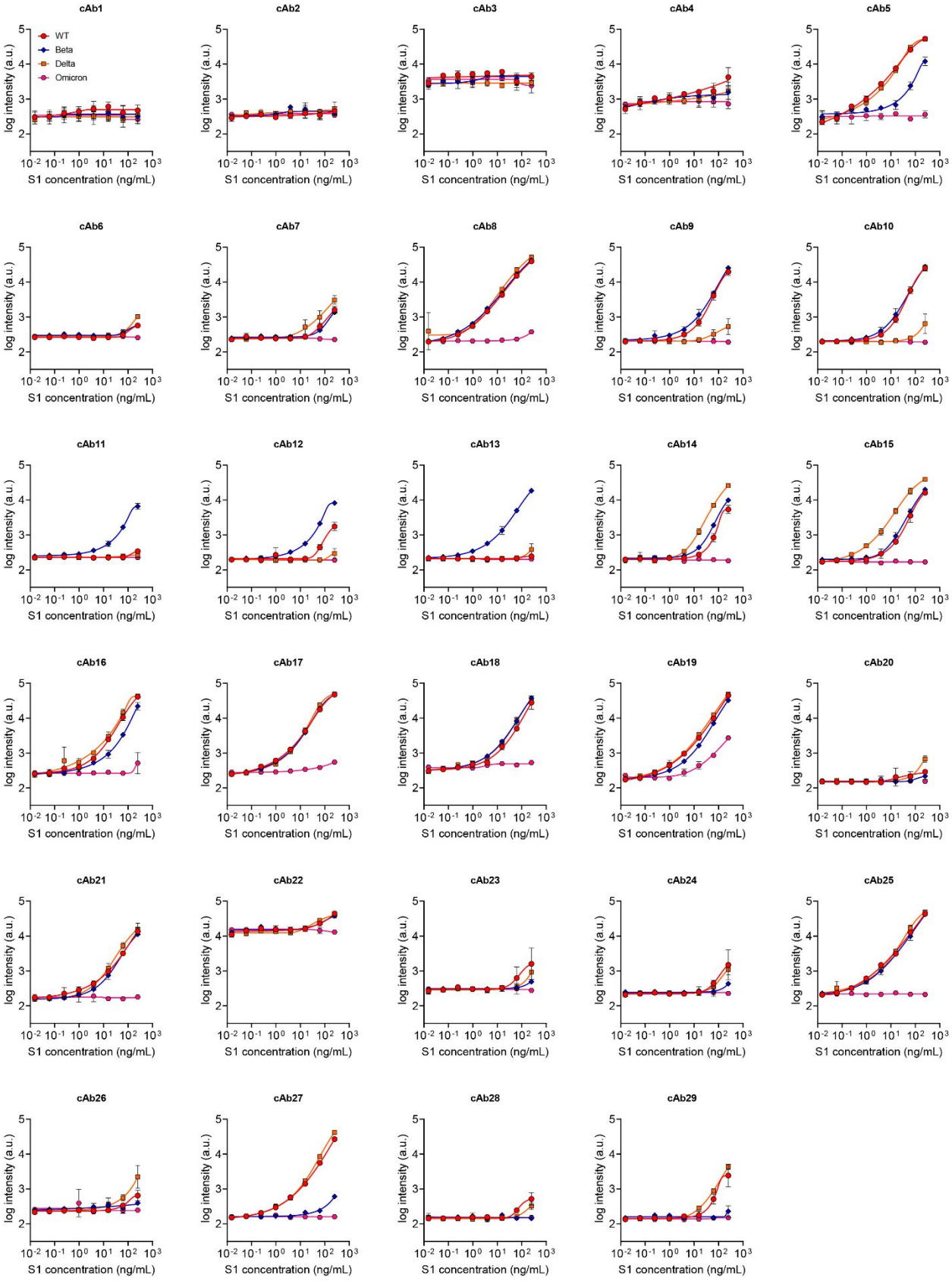
cAb1
cAb2
cAb3
cAb4
cAb5
cAb6
cAb7
cAb8
cAb9
cAb10
cAb11
cAb12
cAb13
cAb14
cAb15
cAb16
cAb17
cAb18
cAb19
cAb20
cAb21
cAb22
cAb23
cAb24
cAb25
cAb26
cAb27
cAb28
cAb29
WT
Beta
Delta
Omicron
log intensity (a.u.)
S1 concentration (ng/mL)

dAb7

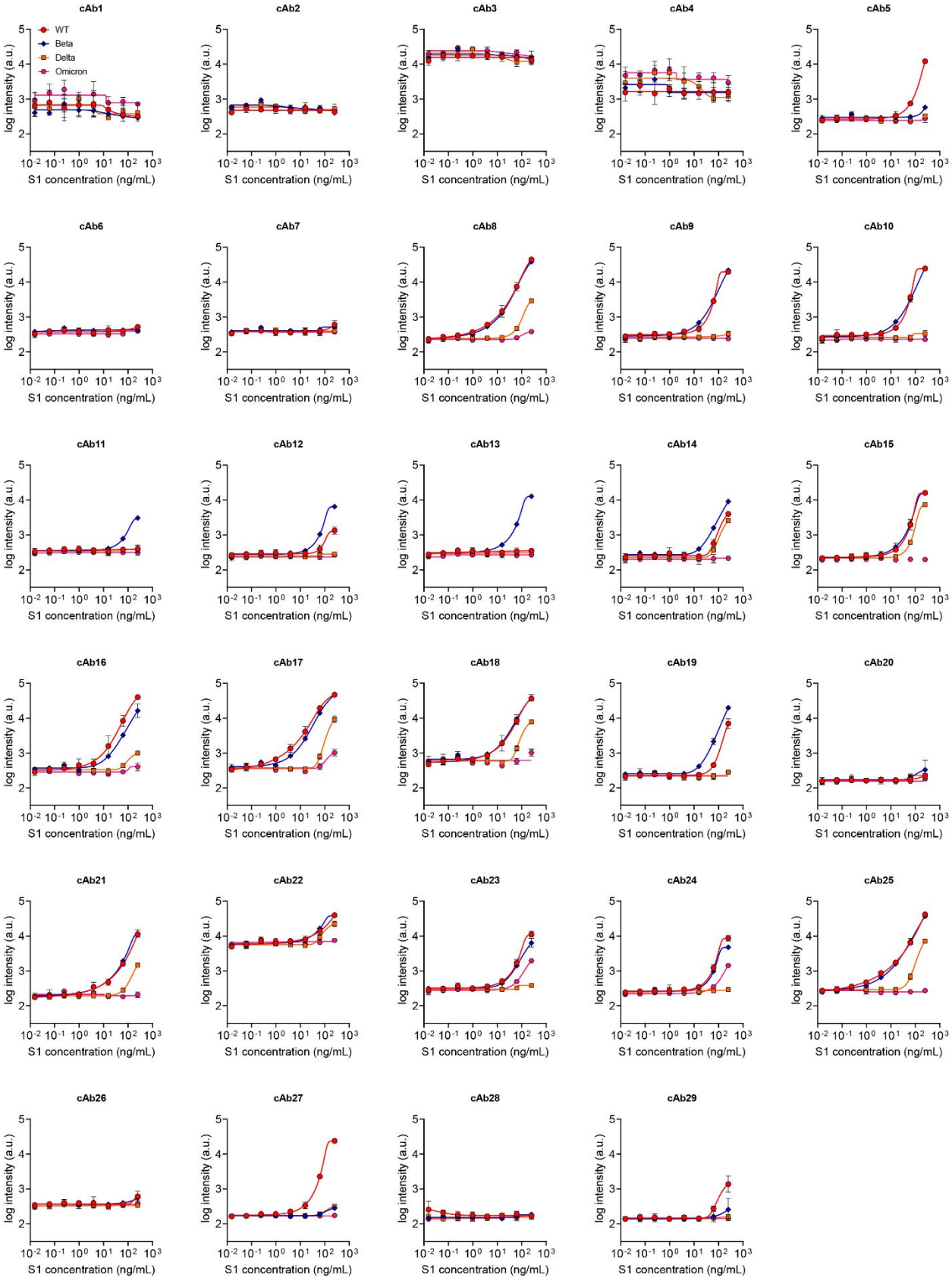
cAb1
cAb2
cAb3
cAb4
cAb5
cAb6
cAb7
cAb8
cAb9
cAb10
cAb11
cAb12
cAb13
cAb14
cAb15
cAb16
cAb17
cAb18
cAb19
cAb20
cAb21
cAb22
cAb23
cAb24
cAb25
cAb26
cAb27
cAb28
cAb29
WT
Beta
Delta
Omicron
log intensity (a.u.)
S1 concentration (ng/mL)

dAb8

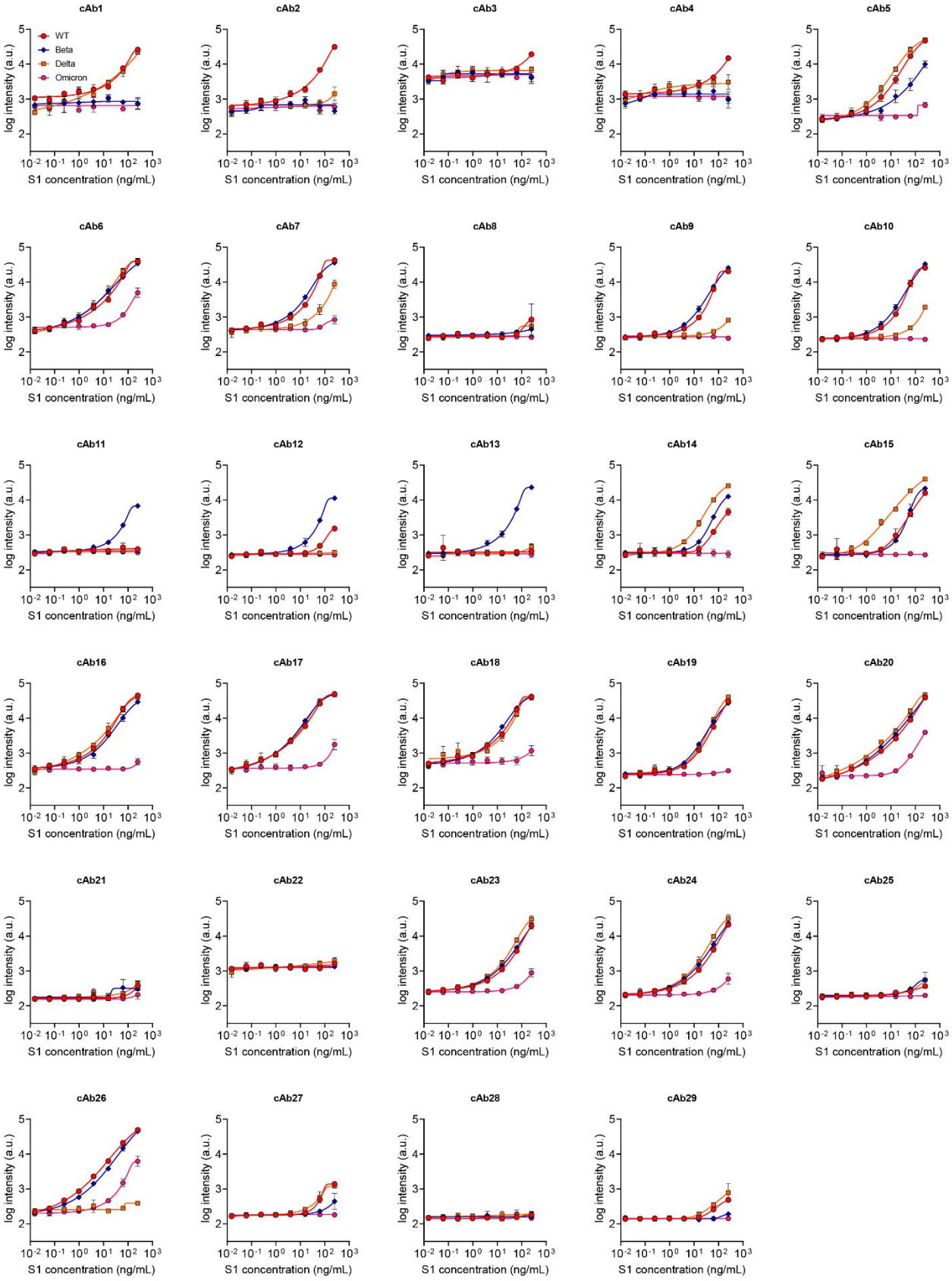
cAb1
cAb2
cAb3
cAb4
cAb5
cAb6
cAb7
cAb8
cAb9
cAb10
cAb11
cAb12
cAb13
cAb14
cAb15
cAb16
cAb17
cAb18
cAb19
cAb20
cAb21
cAb22
cAb23
cAb24
cAb25
cAb26
cAb27
cAb28
cAb29
WT
Beta
Delta
Omicron
log intensity (a.u.)
S1 concentration (ng/mL)

dAb11

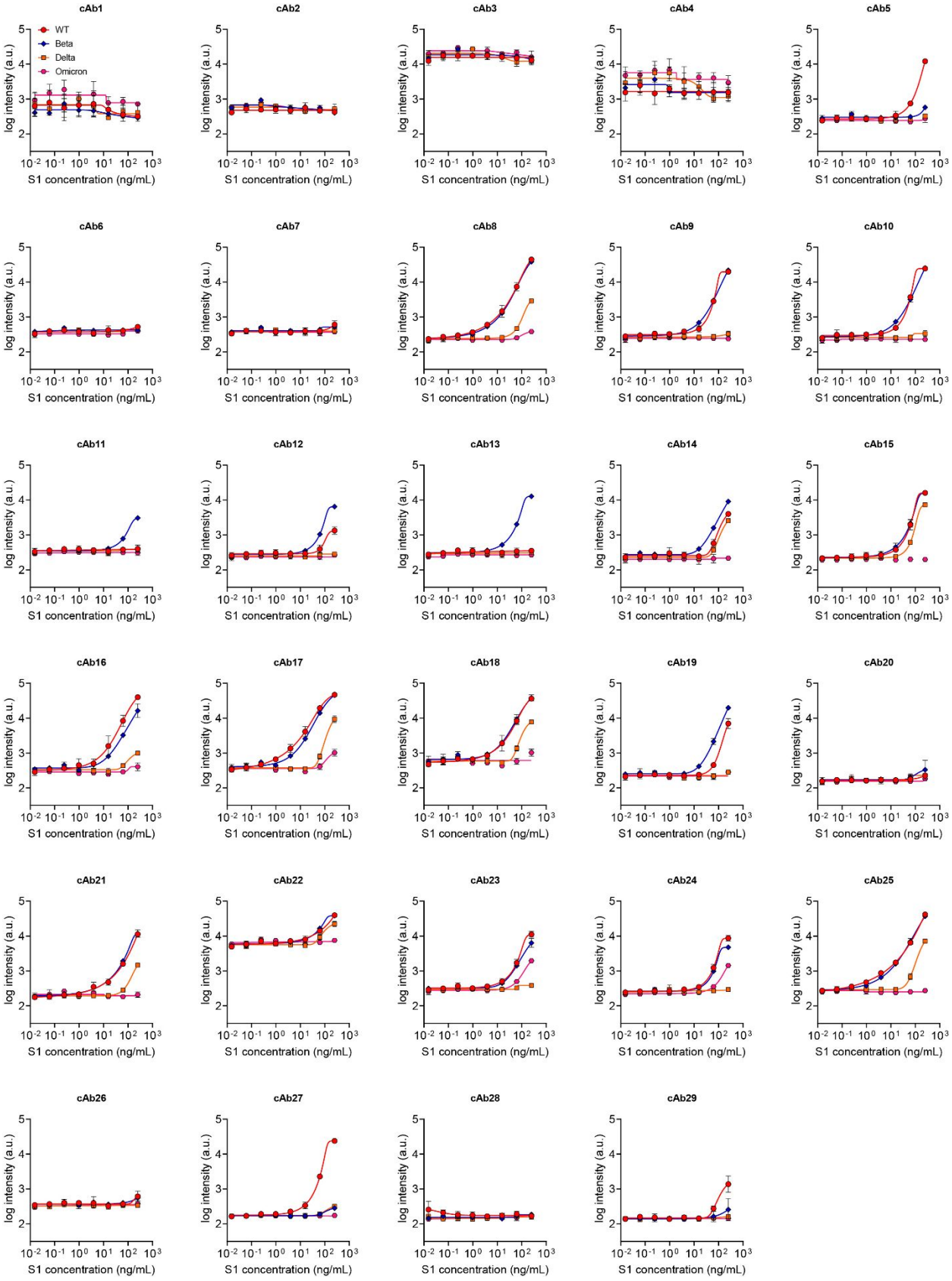
cAb1
cAb2
cAb3
cAb4
cAb5
cAb6
cAb7
cAb8
cAb9
cAb10
cAb11
cAb12
cAb13
cAb14
cAb15
cAb16
cAb17
cAb18
cAb19
cAb20
cAb21
cAb22
cAb23
cAb24
cAb25
cAb26
cAb27
cAb28
cAb29
WT
Beta
Delta
Omicron
log intensity (a.u.)
S1 concentration (ng/mL)

dAb13

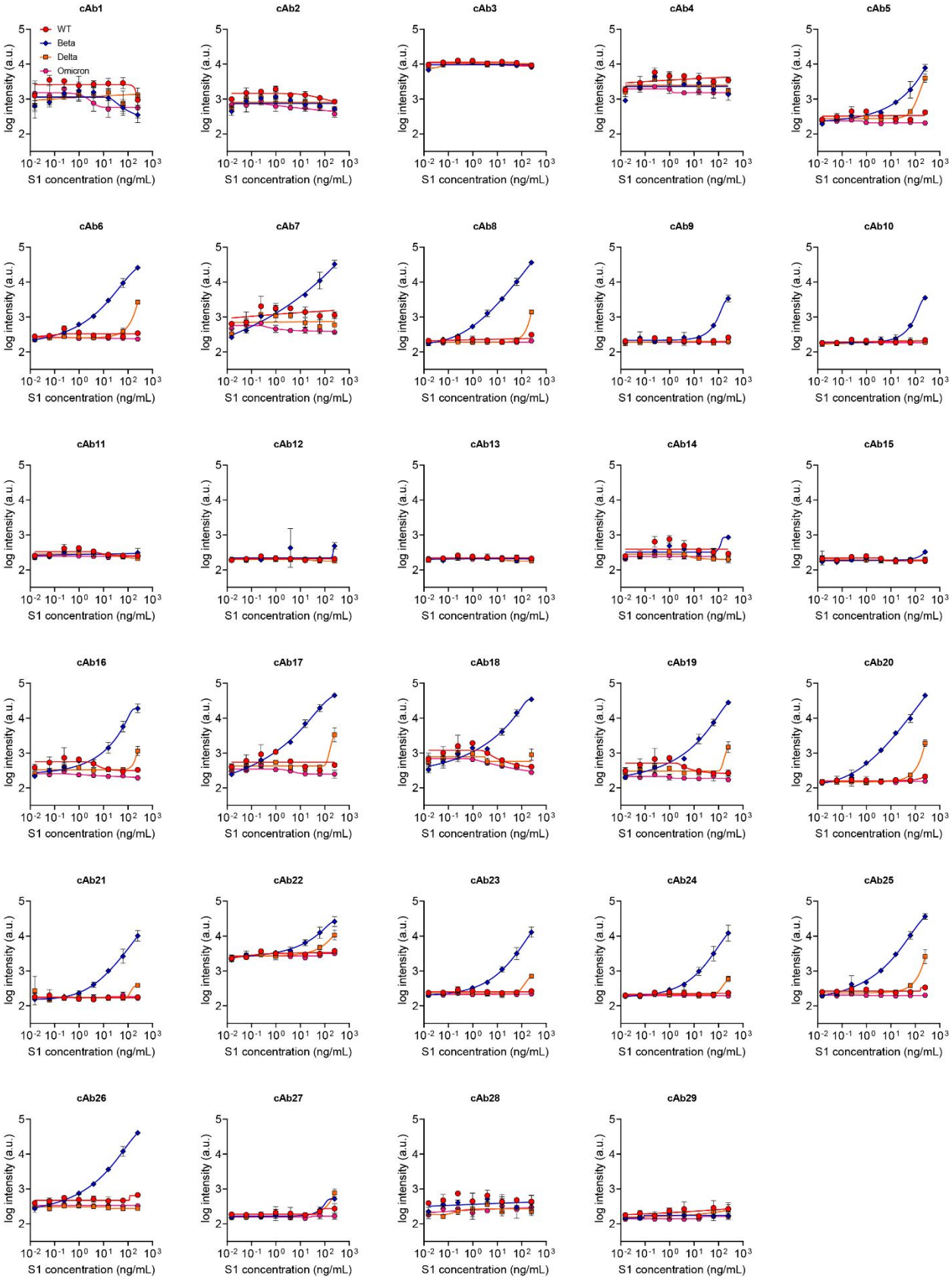
cAb1
cAb2
cAb3
cAb4
cAb5
cAb6
cAb7
cAb8
cAb9
cAb10
cAb11
cAb12
cAb13
cAb14
cAb15
cAb16
cAb17
cAb18
cAb19
cAb20
cAb21
cAb22
cAb23
cAb24
cAb25
cAb26
cAb27
cAb28
cAb29
WT
Beta
Delta
Omicron
log intensity (a.u.)
S1 concentration (ng/mL)

dAb16

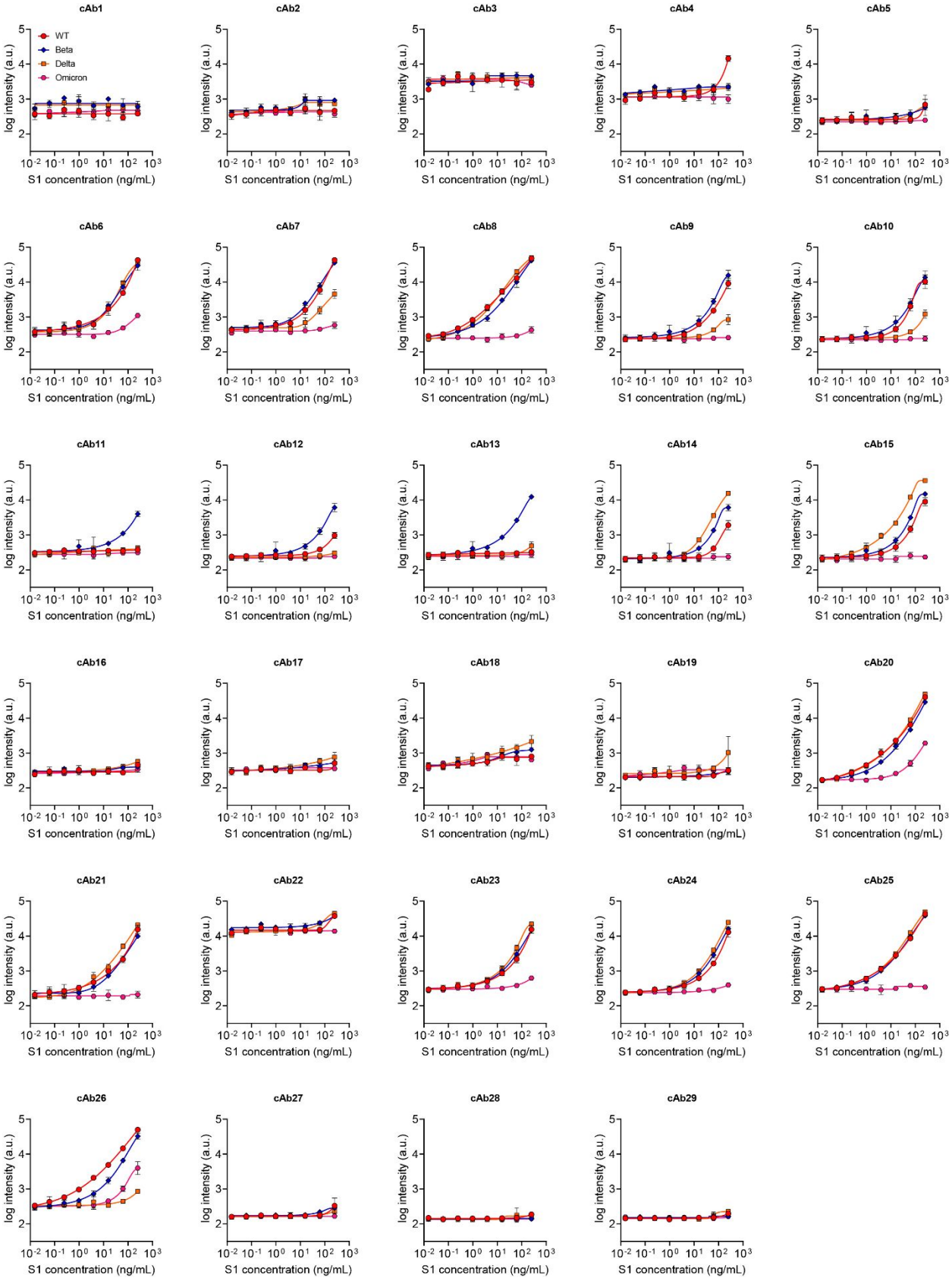
cAb1
cAb2
cAb3
cAb4
cAb5
cAb6
cAb7
cAb8
cAb9
cAb10
cAb11
cAb12
cAb13
cAb14
cAb15
cAb16
cAb17
cAb18
cAb19
cAb20
cAb21
cAb22
cAb23
cAb24
cAb25
cAb26
cAb27
cAb28
cAb29
WT
Beta
Delta
Omicron
log intensity (a.u.)
S1 concentration (ng/mL)

dAb17

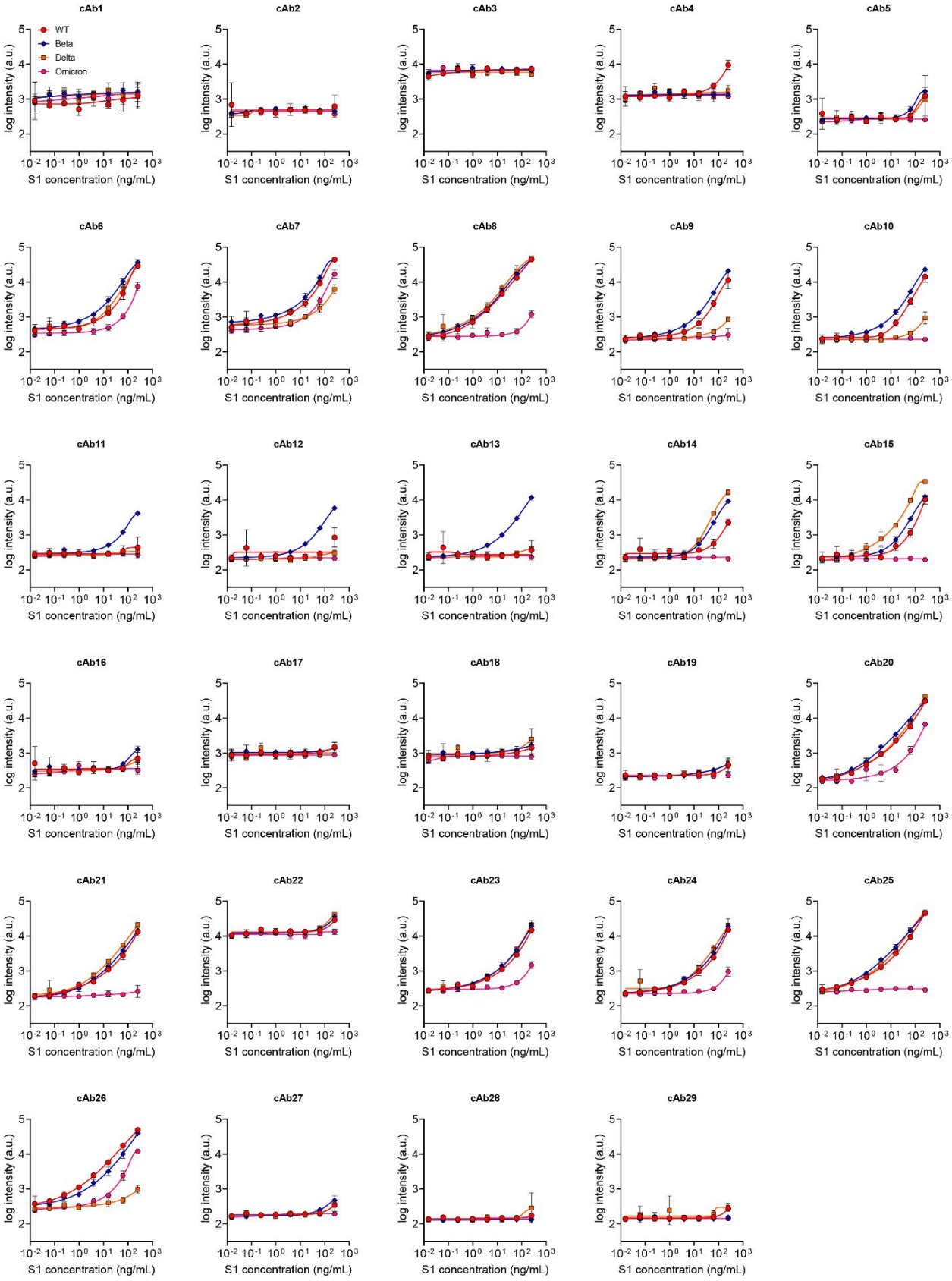
cAb1
cAb2
cAb3
cAb4
cAb5
cAb6
cAb7
cAb8
cAb9
cAb10
cAb11
cAb12
cAb13
cAb14
cAb15
cAb16
cAb17
cAb18
cAb19
cAb20
cAb21
cAb22
cAb23
cAb24
cAb25
cAb26
cAb27
cAb28
cAb29
WT
Beta
Delta
Omicron
log intensity (a.u.)
S1 concentration (ng/mL)

dAb18

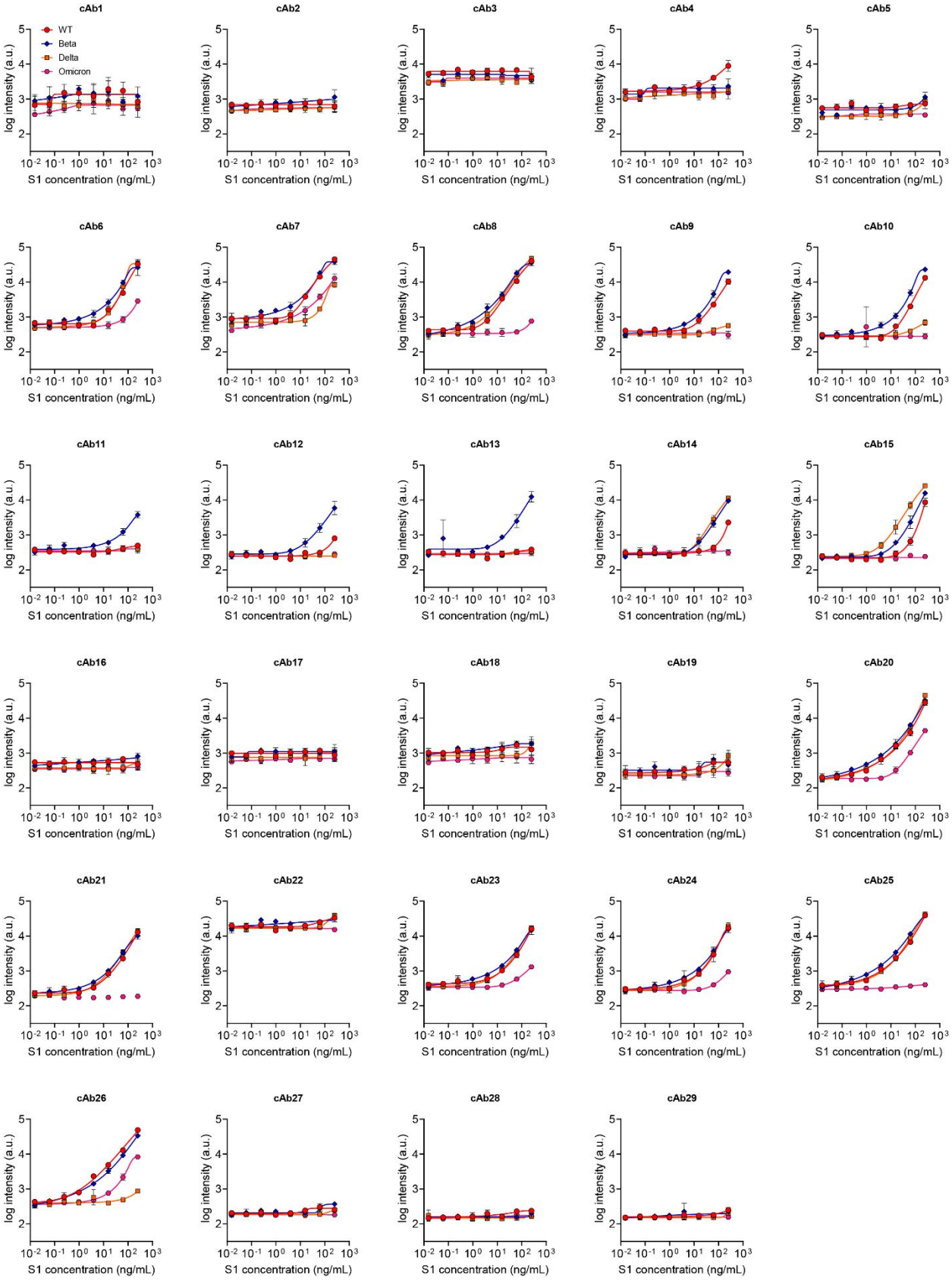
cAb1
cAb2
cAb3
cAb4
cAb5
cAb6
cAb7
cAb8
cAb9
cAb10
cAb11
cAb12
cAb13
cAb14
cAb15
cAb16
cAb17
cAb18
cAb19
cAb20
cAb21
cAb22
cAb23
cAb24
cAb25
cAb26
cAb27
cAb28
cAb29
WT
Beta
Delta
Omicron
log intensity (a.u.)
S1 concentration (ng/mL)

dAb19

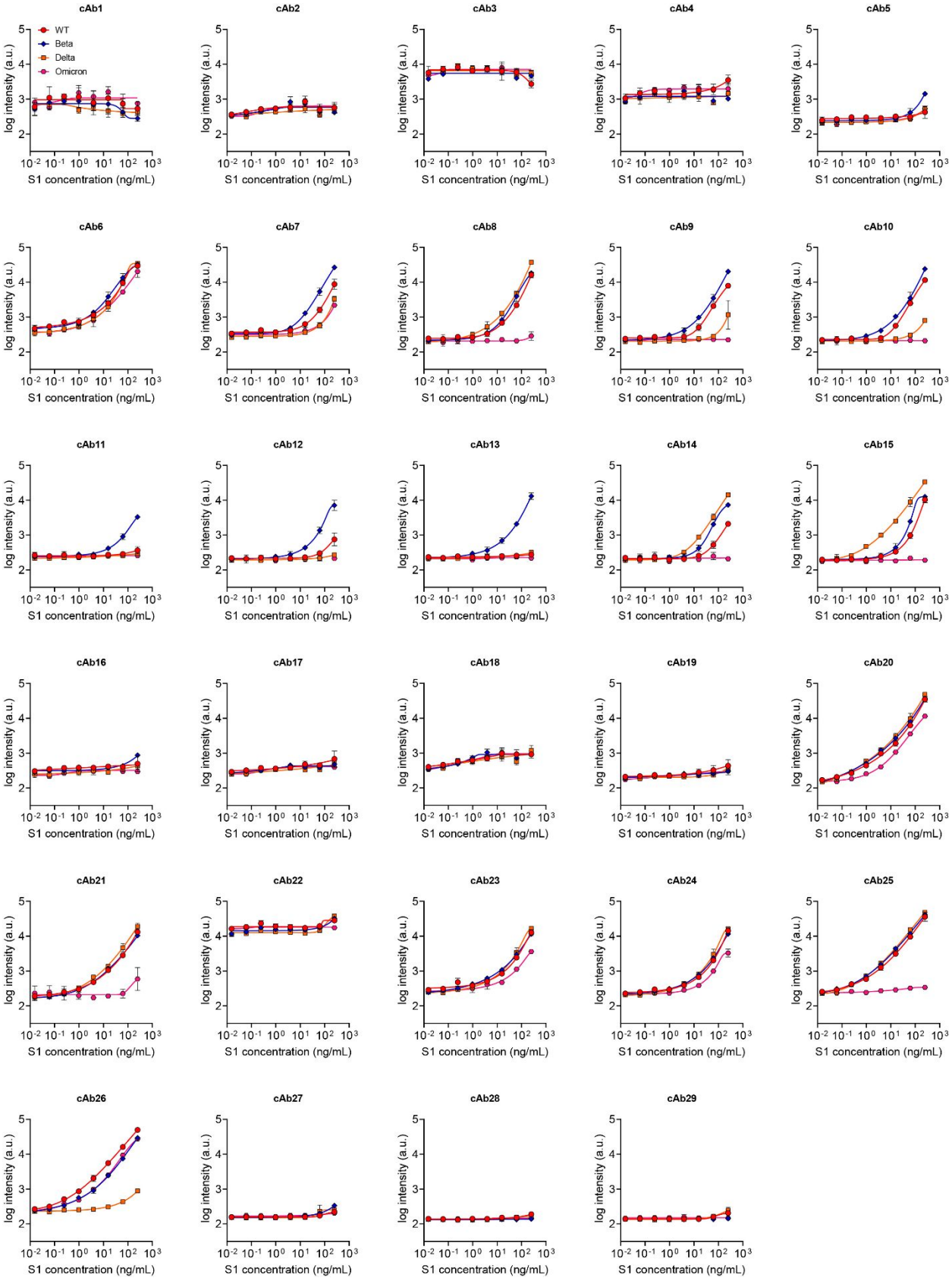
cAb1
cAb2
cAb3
cAb4
cAb5
cAb6
cAb7
cAb8
cAb9
cAb10
cAb11
cAb12
cAb13
cAb14
cAb15
cAb16
cAb17
cAb18
cAb19
cAb20
cAb21
cAb22
cAb23
cAb24
cAb25
cAb26
cAb27
cAb28
cAb29
WT
Beta
Delta
Omicron
log intensity (a.u.)
S1 concentration (ng/mL)

dAb20

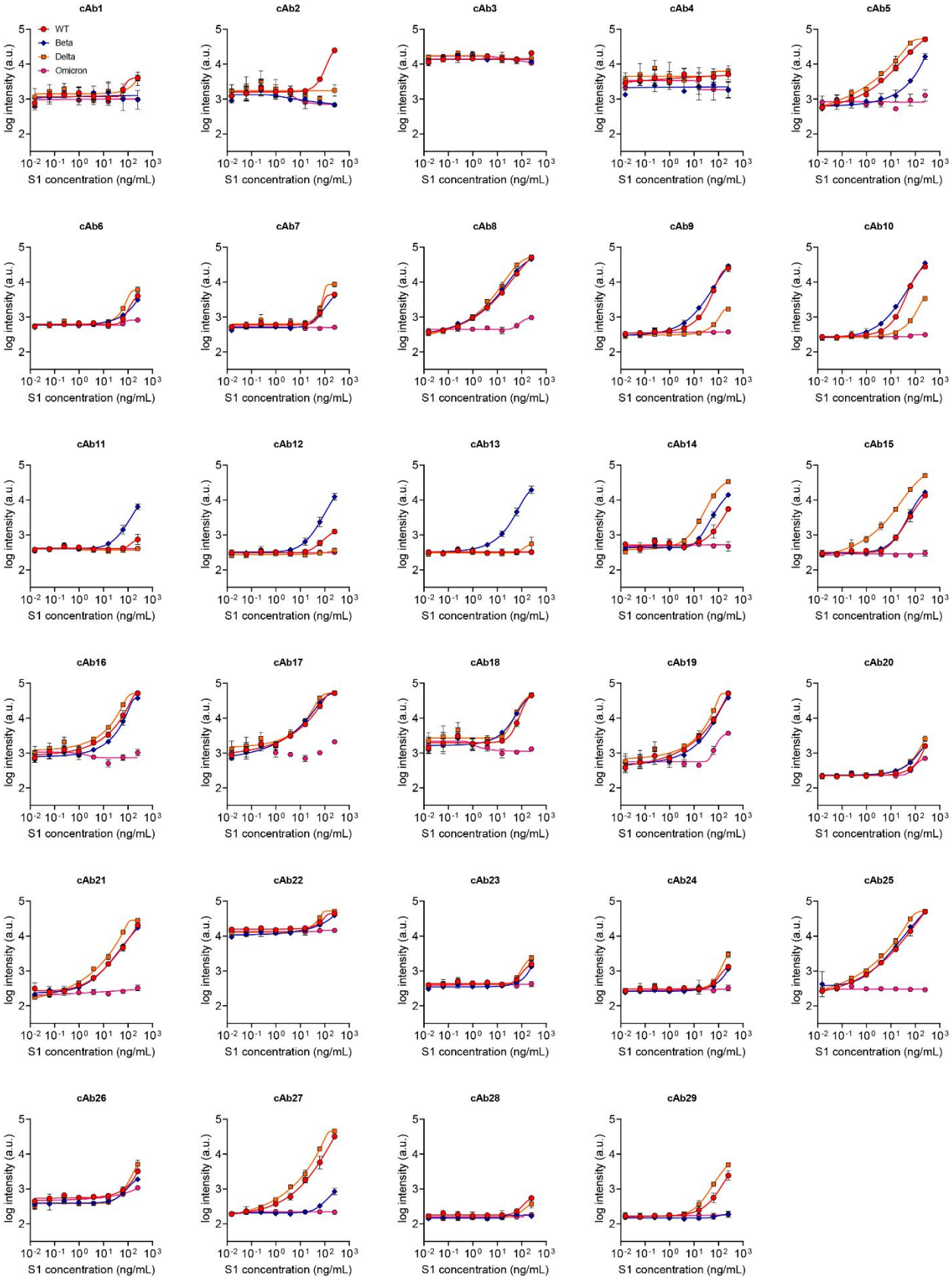
cAb1
cAb2
cAb3
cAb4
cAb5
cAb6
cAb7
cAb8
cAb9
cAb10
cAb11
cAb12
cAb13
cAb14
cAb15
cAb16
cAb17
cAb18
cAb19
cAb20
cAb21
cAb22
cAb23
cAb24
cAb25
cAb26
cAb27
cAb28
cAb29
WT
Beta
Delta
Omicron
log intensity (a.u.)
S1 concentration (ng/mL)

dAb25

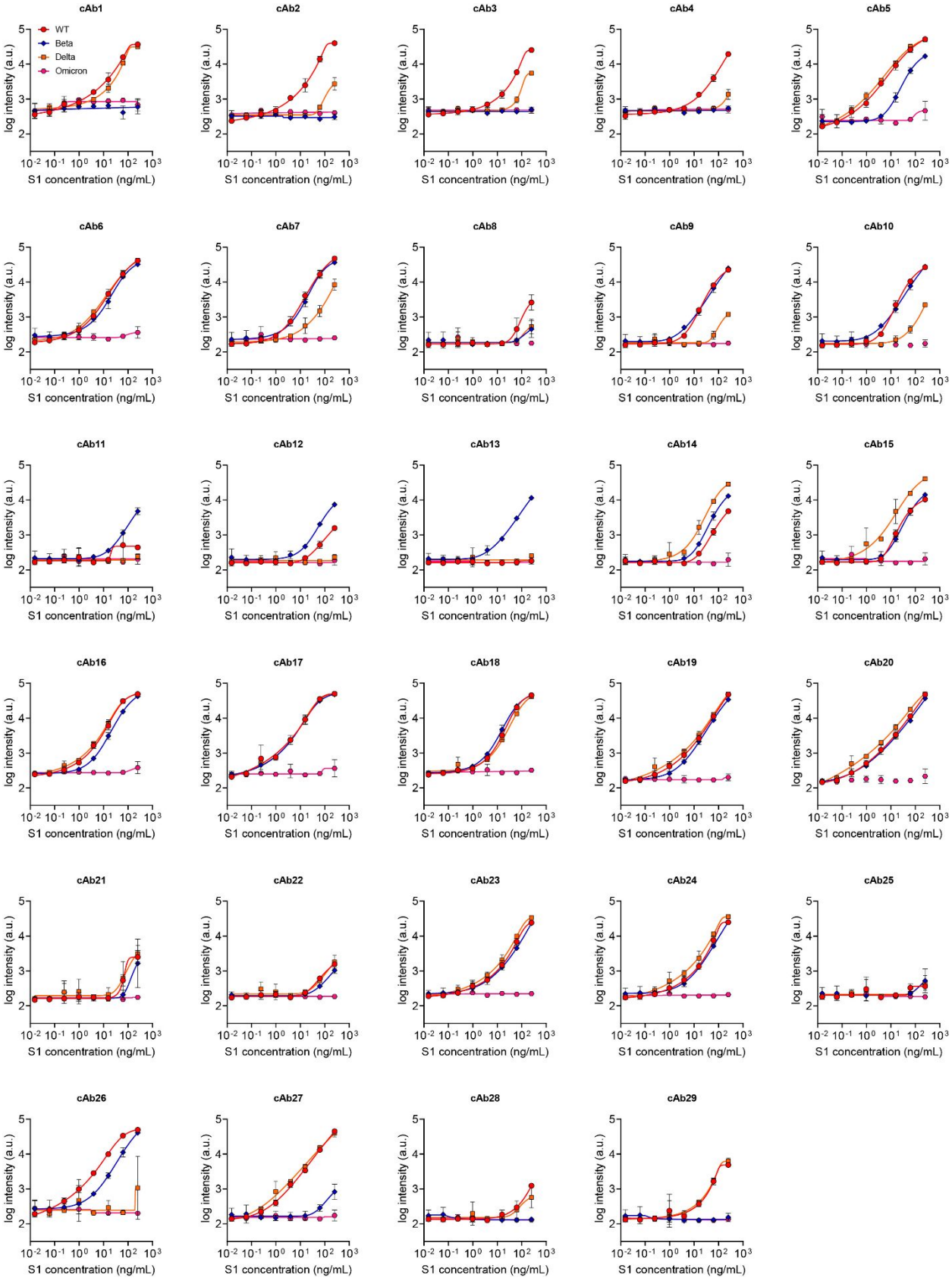
cAb1
cAb2
cAb3
cAb4
cAb5
cAb6
cAb7
cAb8
cAb9
cAb10
cAb11
cAb12
cAb13
cAb14
cAb15
cAb16
cAb17
cAb18
cAb19
cAb20
cAb21
cAb22
cAb23
cAb24
cAb25
cAb26
cAb27
cAb28
cAb29
WT
Beta
Delta
Omicron
log intensity (a.u.)
S1 concentration (ng/mL)

Figure S1. High-throughput anti-SARS-CoV-2 S protein antibody screen on the D4, where 29 cAbs were tested against 13 Alexa Fluor 647 labeled dAbs. For each combination, an 8-point dose-response was tested for S1 proteins from 4 SARS-CoV-2 variants: WT, Beta, Delta, and Omicron. In total, 1508 dose-response curves were generated and analyzed.

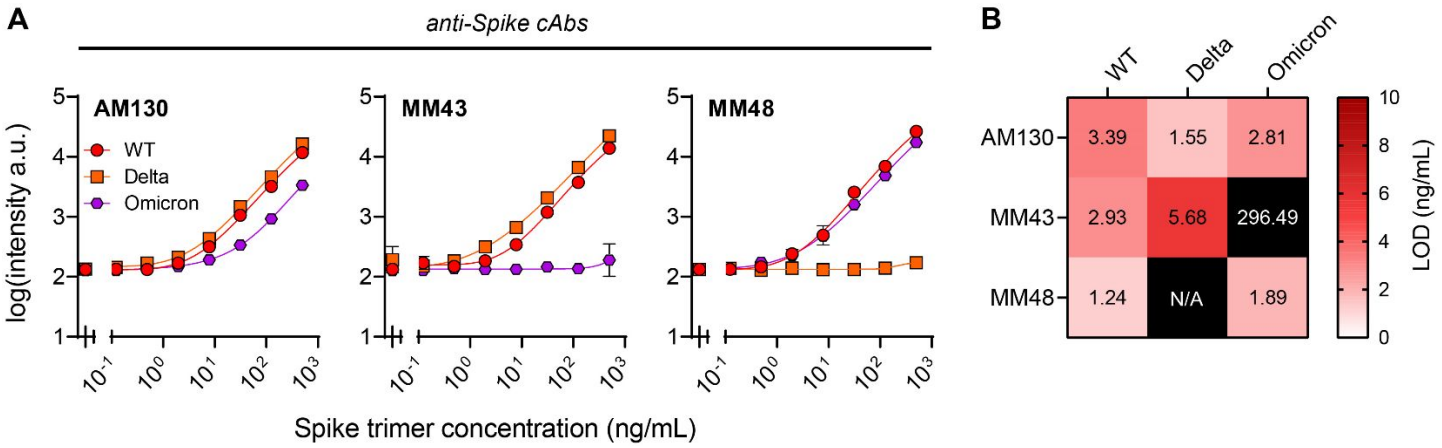

Figure S2. CoVariant-SCAN performance against S trimer. **(A)** Antibodies selected by screening against the S1 domain bind similarly to the S trimer. Like the S1 monomers, an attenuation of signal is observed with MM43 binding to Omicron trimer and MM48 binding to Delta trimer. **(B)** Calculated LODs show that CoVariant-SPOT is slightly less sensitive to S timer as compared to S1 monomer, but the trends between variants remain unchanged.

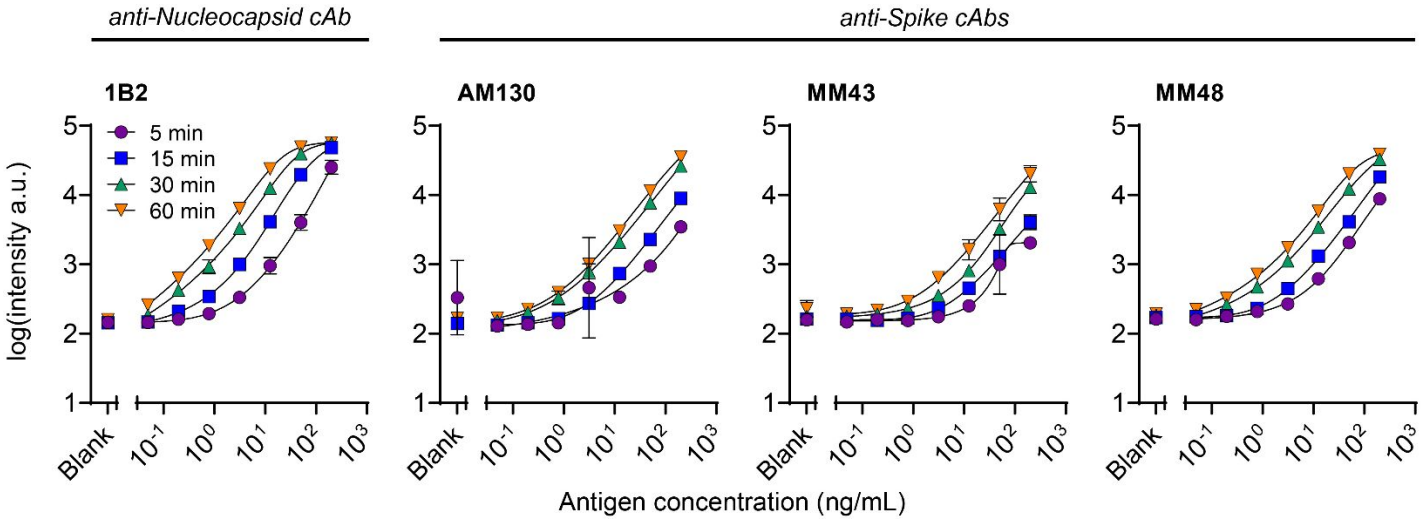

Figure S3. Impact of incubation time. An 8-point dose-response for WT SARS-CoV-2 N and S1 protein was tested at various incubation times. Sensitivity to both N and S1 proteins increased with incubation time for all antibodies, justifying the recommended 60-minute incubation time for CoVariant-SPOT.

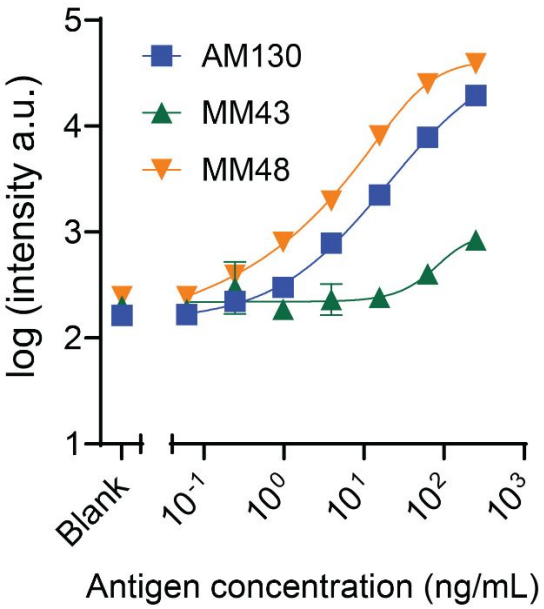

Figure S4. Omicron BA.2 subvariant dose-response on CoVariant-SPOT. CoVariant-SPOT maintains a similar sensitivity to the BA.2 subvariant as compared to the standard sublineage (BA.1). Attenuation of MM43 dose-response is observed.

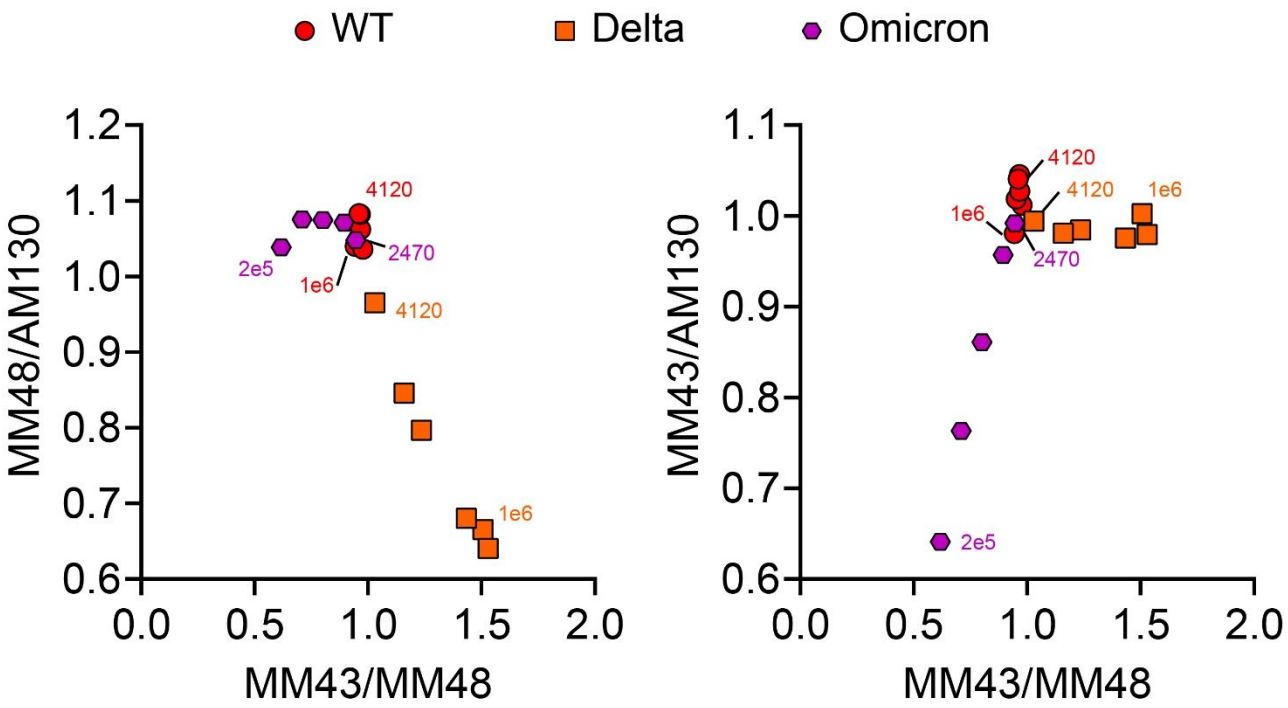

Figure S5. Anti-S cAb ratios to differentiate between WT, Delta, and Omicron variants in UV inactivated viruses. Numbers in the graph represent the concentration of the isolates ($TCID_{50}$/mL). Differentiation improves at higher virus concentrations.

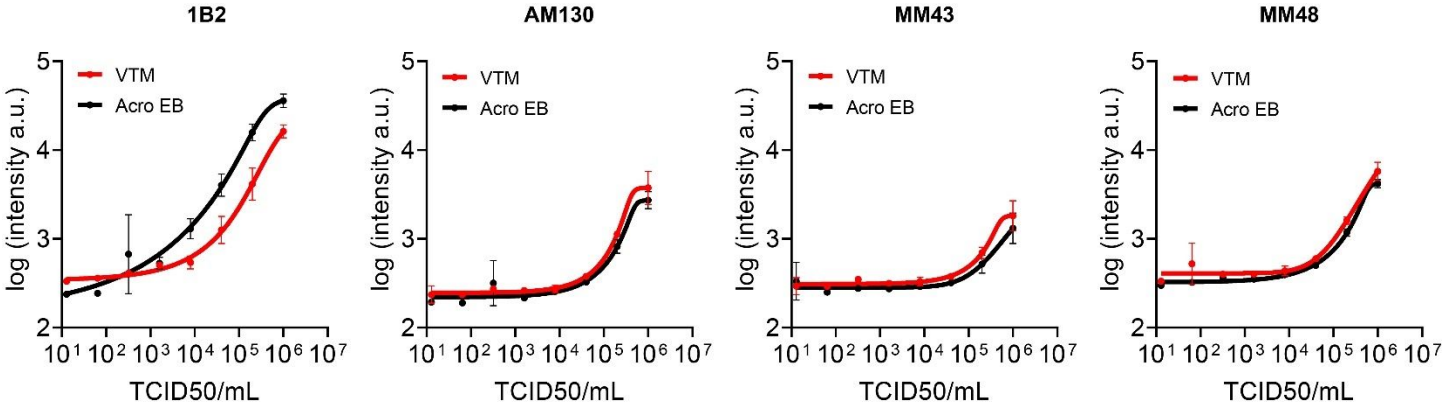

Figure S6. Comparison of VTM (Redoxica, VTM-500mL) and Acro Biosystems extraction/lysis buffer (catalog number: LY14) to detect N protein and S protein from WT SARS-CoV-2 isolates (ZeptoMetrix). Each data point represents the average of two replicates, with SD shown. Furthest left data point is a blank. Legend 1B2: cAb used for N protein detection; AM130, MM43 and MM48 are the three different cAb's used for VOC discrimination based on S protein detection.

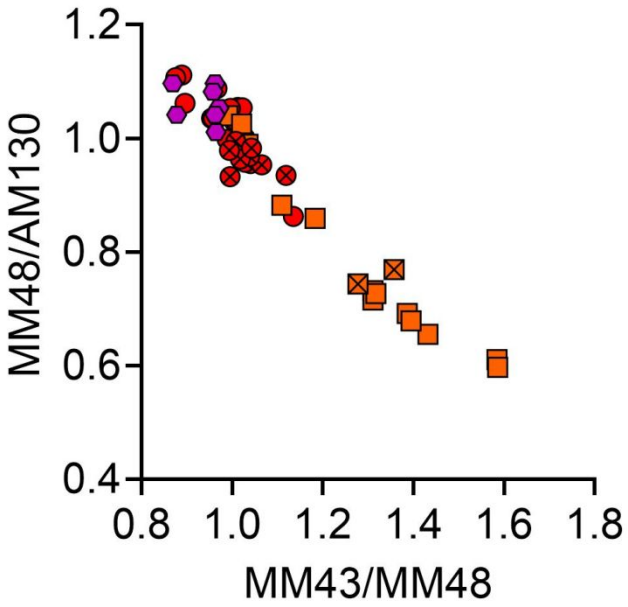

Figure S7. Anti-S cAb ratios to differentiate between WT-like, Delta, and Omicron for all positive COVID-19 samples with 1B2 intensity greater than 2.72 arbitrary units. Samples with an “x” have not been sequenced but are presumed to be a given variant based on sample collection date. WT sample lineages are defined in Table S1.

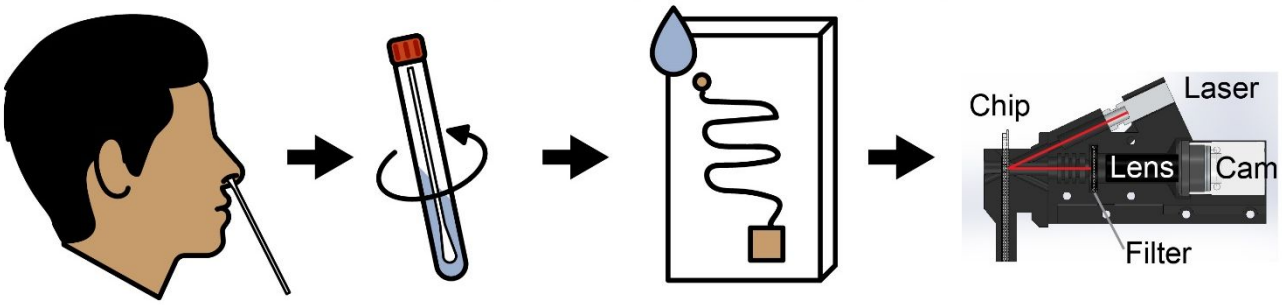

Figure S8. Schematic of workflow for POC testing, where a nasal swab is added to lysis/extraction buffer, sample is added by dropper to the microfluidic cassette which automates the assay. Finally, the cassette is imaged on the D4Scope detector.

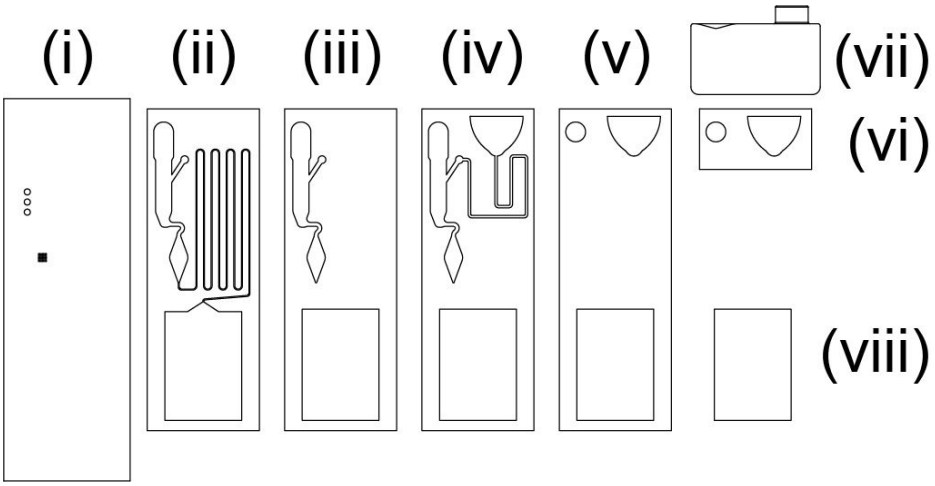

Figure S9. Exploded view of the microfluidic CoVariant-SPOT cassette. (i) Base POEGMA coated glass with inkjet printed reagents. (ii) First adhesive layer that creates the (TC) side walls and includes the profile of the (RC) and (WP). (iii) First acrylic layer that seals the (TC) and gives the (RC) it's depth to accommodate the sample volume. (iv) Second adhesive layer that creates the delay channel for the (WB) that ensures sample has settled into the (RC) prior to wash buffer introduction into the (RC). It also maintains the (RC) profile to ensure an optically transparent line-of-sight for D4Scope imaging. (v) Second acrylic layer that seals off the (RC) and wash delay channel while maintaining access for the (SI) and (WB). (vi) Adhesive backing that attaches the inlet reservoir. (vii) 3D printed inlet reservoir where sample and wash buffer are added. (viii) (WP).

Table S1. Clinical sample summary.

#	Source	Subject ID	Draw Date (M/Y)	Age	Gender	PCR Result	PCR test method	Viral load (copies/mL)	Lineage
1	MESSI	7AC7BA	Jan-21	32	Female	Negative	Method 2	N/A	N/A
2	MESSI	322088	Jan-21	79	Female	Negative	Method 2	N/A	N/A
3	MESSI	025CBE	Jan-21	83	Male	Negative	Method 2	N/A	N/A
4	MESSI	DA8A0E	Jan-21	53	Male	Negative	Method 2	N/A	N/A
5	MESSI	1DEB9C	Jun-20	62	Female	Negative	Method 1	N/A	N/A
6	MESSI	9759E7	Jul-20	70	Male	Negative	Method 1	N/A	N/A
7	MESSI	48298F	Aug-20	17	Male	Negative	Method 1	N/A	N/A
8	MESSI	D1D8AC	Nov-20	60	Male	Negative	Method 1	N/A	N/A
9	MESSI	FF27EC	Oct-21	33	Male	Negative	Method 2	N/A	N/A
10	MESSI	4A2671	Oct-21	47	Male	Negative	Method 2	N/A	N/A
11	MESSI	ADAF6C	Oct-21	46	Male	Negative	Method 2	N/A	N/A
12	MESSI	5217A5	Oct-21	54	Male	Negative	Method 2	N/A	N/A
13	MESSI	D234DB	Oct-21	36	Female	Negative	Method 2	N/A	N/A
14	MESSI	ABF76B	Oct-21	36	Male	Negative	Method 2	N/A	N/A
15	MESSI	D41350	Dec-21	44	Female	Negative	Method 2	N/A	N/A
16	MESSI	D41350	Oct-21	44	Female	Negative	Method 2	N/A	N/A
17	MESSI	00D120	Dec-21	50	Male	Negative	Method 2	N/A	N/A
18	MESSI	E48FF4	Dec-21	53	Male	Negative	Method 2	N/A	N/A
19	MESSI	E24969	Dec-21	56	Male	Negative	Method 2	N/A	N/A
20	MESSI	2D814B	Dec-21	51	Male	Negative	Method 2	N/A	N/A
21	MESSI	CE4D04	Dec-21	19	Male	Negative	Method 2	N/A	N/A
22	MESSI	C421AD	Dec-21	19	Female	Negative	Method 2	N/A	N/A
23	MESSI	3E7475	Jan-22	25	Male	Negative	Method 2	N/A	N/A
24	MESSI	F7190B	Jan-22	42	Female	Negative	Method 2	N/A	N/A
25	MESSI	72BF40	Jan-22	53	Male	Negative	Method 2	N/A	N/A
26	MESSI	8FDB69	Jan-22	42	Male	Negative	Method 2	N/A	N/A
27	MESSI	FEC4E9	Jan-22	47	Male	Negative	Method 2	N/A	N/A
28	MESSI	02608B	Jan-22	56	Male	Negative	Method 2	N/A	N/A
29	MESSI	2566E0	Jan-22	54	Female	Negative	Method 2	N/A	N/A
30	MESSI	B4AA7C	Jan-22	59	Male	Negative	Method 2	N/A	N/A
31	MESSI	ED6824	Feb-22	55	Male	Negative	Method 2	N/A	N/A
32	MESSI	150B4B	Feb-22	40	Male	Negative	Method 2	N/A	N/A
33	DLS	KH21-18559	Nov-21	58	Female	Positive	Abbott RealTime SARS-CoV-2 (RT)-PCR	N/A	N/A
34	DLS	KH21-18560	Nov-21	37	Male	Positive	Abbott RealTime SARS-CoV-2 (RT)-PCR	N/A	N/A
35	DLS	KH21-18564	Nov-21	55	Male	Positive	Abbott RealTime SARS-CoV-2 (RT)-PCR	N/A	N/A
36	DLS	KH21-18561	Nov-21	47	Male	Positive	Abbott RealTime	N/A	N/A

							SARS-CoV-2 (RT)-PCR		
37	DLS	KH20-36735	Mar-20	67	Female	Positive	Abbott RealTime SARS-CoV-2 (RT)-PCR	N/A	N/A
38	DLS	KH20-12011	Apr-20	60	Male	Positive	Abbott RealTime SARS-CoV-2 (RT)-PCR	N/A	N/A
39	DLS	KH20-62850	May-20	65	Female	Positive	PerkinElmer Applied Biosystems 7500	N/A	N/A
40	DLS	KH20-71092	Apr-20	65	Male	Positive	PerkinElmer Applied Biosystems 7500	N/A	N/A
41	DLS	KH20-71564	Apr-20	41	Male	Positive	PerkinElmer Applied Biosystems 7500	N/A	N/A
42	DLS	KH20-78468	Nov-20	30	Female	Positive	Thermo Fisher	N/A	N/A
43	DLS	KH20-75153	Apr-20	66	Male	Positive	PerkinElmer Applied Biosystems 7500	N/A	N/A
44	DLS	KH20-61677	Apr-20	81	Female	Positive	PerkinElmer Applied Biosystems 7500	N/A	N/A
45	DLS	KH20-61634	Apr-20	54	Female	Positive	PerkinElmer Applied Biosystems 7500	N/A	N/A
46	DLS	KH20-71078	Apr-20	65	Female	Positive	PerkinElmer Applied Biosystems 7500	N/A	N/A
47	MESSI	C2C669	Apr-20	39	Female	Positive	Method 1	1356918328	B.1
48	MESSI	A0F8B9	Apr-20	22	Male	Positive	Method 1	88384	Unassigned
49	MESSI	2812A3	Apr-20	52	Male	Positive	Method 1	11363	Unassigned
50	MESSI	3EA6A0	May-20	35	Female	Positive	Method 1	152273099	B.1
51	MESSI	4DFE6A	May-20	30	Male	Positive	Method 1	2661	B.1
52	MESSI	AA3F84	Jun-20	19	Male	Positive	Method 2	3989154	B.1.521
53	MESSI	598A88	Jun-20	27	Female	Positive	Method 1	113824	B.1.1.231
54	MESSI	7C2A2A	Jul-20	62	Female	Positive	Method 1	10800000	B.1.1.148
55	MESSI	2F0D5E	Jul-20	59	Male	Positive	Method 1	10400	B.1
56	MESSI	C31FF9	Aug-20	78	Male	Positive	Method 1	12900000	B.1
57	MESSI	78DDF0	Aug-20	65	Female	Positive	Method 1	31200	B.1.1.135
58	MESSI	29EEF5	Aug-20	44	Female	Positive	Method 1	48200	B.1.240
59	MESSI	B63F74	Sep-20	65	Female	Positive	Method 1	100000	B.1.2
60	MESSI	00D120	Nov-20	50	Male	Positive	Method 2	408325	B.1.2
61	MESSI	76366E	Jan-21	69	Female	Positive	Method 2	957199	B.1.2
62	MESSI	FFE532	Dec-20	63	Male	Positive	Method 2	185184356	B.1.2
63	MESSI	3501A9	Jan-21	25	Female	Positive	Method 2	14282316	B.1

64	MESSI	5217A5	Sep-21	54	Male	Positive	Method 2	81313	AY.44
65	MESSI	A8FD53	Feb-21	34	Female	Positive	Method 2	3363873	B.1.2
66	MESSI	B4D0DE	Feb-21	63	Male	Positive	Method 2	48304	B.1.1.207
67	MESSI	7400BF	Feb-21	48	Female	Positive	Method 2	602458286	B.1.2
68	MESSI	B2905A	Feb-21	63	Female	Positive	Method 2	9008908	B.1.1.207
69	MESSI	E60E94	Feb-21	15	Female	Positive	Method 2	5755536	B.1.2
70	MESSI	67B41D	Feb-21	15	Female	Positive	Method 2	276176054	B.1.2
71	MESSI	C795F1	Feb-21	53	Male	Positive	Method 2	4605960	B.1.2
72	MESSI	8CF0CC	May-21	33	Female	Positive	Method 2	1217247	B.1.526
73	MESSI	FB394D	May-21	14	Male	Positive	Method 2	2714713	B.1.526
74	MESSI	17A783	Aug-21	33	Female	Positive	Method 2	692489	AY.118
75	MESSI	9E259D	Aug-21	31	Male	Positive	Method 1	94408300	AY.118
76	MESSI	9FAB68	Sep-21	66	Male	Positive	Method 1	276926644	AY.103
77	MESSI	E55DCE	Sep-21	31	Male	Positive	Method 1	53113968	AY.103
78	MESSI	EB2A47	Sep-21	54	Male	Positive	Method 2	438627835	AY.44
79	MESSI	85F0AB	Sep-21	51	Male	Positive	Method 2	138749	AY.103
80	MESSI	C9EEEA	Sep-21	37	Male	Positive	Method 2	4991978	AY.44
81	MESSI	ADAF6C	Sep-21	46	Male	Positive	Method 2	200625	AY.44
82	MESSI	3E8F04	Sep-21	35	Male	Positive	Method 2	67287	AY.103
83	MESSI	1E4BD7	Sep-21	44	Male	Positive	Method 2	417455	AY.44
84	MESSI	8655BF	Sep-21	38	Male	Positive	Method 2	8638159	AY.44
85	MESSI	EE435A	Sep-21	48	Male	Positive	Method 2	1600293	AY.103
86	MESSI	990CA3	Sep-21	67	Male	Positive	Method 2	38730392	AY.103
87	MESSI	845B87	Sep-21	58	Male	Positive	Method 2	37300	AY.103
88	MESSI	A97D5B	Sep-21	27	Male	Positive	Method 2	1298723761	AY.54
89	MESSI	FF27EC	Sep-21	33	Male	Positive	Method 2	436237230	AY.44
90	MESSI	22D142	Aug-21	53	Male	Positive	Method 2	74000519	AY.118
91	MESSI	DE7C56	Jul-21	57	Male	Positive	Method 2	13924	AY.118
92	MESSI	D41350	Jul-21	44	Female	Positive	Method 2	100580235	AY.118
93	MESSI	0F6E02	Apr-21	36	Female	Positive	Method 2	273803376	B.1.2
94	MESSI	02608B	Jan-22	56	Male	Positive	Method 2	50325	BA.1.20
95	MESSI	F7190B	Jan-22	42	Female	Positive	Method 1	353829	BA.1.1.8
96	MESSI	2566E0	Jan-22	54	Female	Positive	Method 2	382134	BA.1.1.18
97	MESSI	8FDB69	Jan-22	42	Male	Positive	Method 1	110782171	BA.1.1
98	MESSI	3E7475	Jan-22	25	Male	Positive	Method 1	28583	BA.1.1
99	MESSI	FEC4E9	Jan-22	47	Male	Positive	Method 2	5284486	BA.1.1
100	MESSI	72BF40	Jan-22	53	Male	Positive	Method 1	3662	BA.1.1.8
101	MESSI	B5CC01	May-22	56	Female	Positive	N/A	N/A	BA.2.12.1
102	MESSI	ED6824	May-22	49	Female	Positive	N/A	N/A	BA.2.12.1
103	MESSI	ED6824	Jan-22	55	Male	Positive	Method 2	288002	BA.1.1
104	MESSI	B5CC01	Jan-22	48	Male	Positive	Method 2	2024081	BA.1.1
105	MESSI	150B4B	Feb-22	40	Male	Positive	Method 2	34165011	BA.1.1
106	MESSI	9C0AA4	Feb-22	34	Male	Positive	Method 1	87487	BA.1.1
107	MESSI	E674EB	Feb-22	49	Male	Positive	Method 1	9441043	BA.1.1
108	MESSI	12CE1E	Mar-22	51	Female	Positive	Method 1	7230964	BA.1.1

Table S2. Antibodies tested in the S high-throughput screen (Figure S1) which includes 29 anti-S antibodies. Antibodies highlighted in blue were included in CoVariant-SPOT.

Antibody ID	Publication Name	Supplier
1	DH1041	DHVI
2	DH1042	DHVI
3	DH1043	DHVI
4	DH1111	DHVI
5	DH1284	DHVI
6	DH1193	DHVI
7	DH1044	DHVI
8	DH1047	DHVI
9	DH1049	DHVI
10	DH1050.1	DHVI
11	DH1051	DHVI
12	DH0148	DHVI
13	DH1054	DHVI
14	DH1053	DHVI
15	DH1055	DHVI
16	LT8010	Leinco Technologies
17	LT5000	Leinco Technologies
18	LT4000	Leinco Technologies
19	S1N-M122	Acro Biosystems
20	S1N-M130	Acro Biosystems
21	40150-D001	Sino Biological
22	40150-D002	Sino Biological
23	40150-D003	Sino Biological
24	40150-D004	Sino Biological
25	40591-MM43	Sino Biological
26	40591-MM48	Sino Biological
27	40592-R001	Sino Biological
28	40592-R117	Sino Biological
29	40592-R118	Sino Biological

Table S3. Limit of detection comparison for CoVariant-SPOT and the microfluidic CoVariant-SPOT.

	Antibody	Limit of detection (ng/mL)		
		WT	*Delta*	*Omicron*
CoV-SPOT	**1B2**	0.07	0.05	0.07
	AM130	0.12	0.23	1.97
	MM43	0.12	0.06	14.40
	MM48	0.06	28.00	0.43
Microfluidic CoV-SPOT	**1B2**	0.02	0.02	0.08
	AM130	0.20	0.62	2.23
	MM43	0.12	1.48	X
	MM48	0.05	12.13	1.88

x – indicates could not be calculated using the resulting fit

Data S1. Source data (separate file).

Data S2. Source data for Figure S1 (separate file).

Supporting information references

1. Joh, D. Y.; Hucknall, A. M.; Wei, Q.; Mason, K. A.; Lund, M. L.; Fontes, C. M.; Hill, R. T.; Blair, R.; Zimmers, Z.; Achar, R. K.; Tseng, D.; Gordan, R.; Freemark, M.; Ozcan, A.; Chilkoti, A., Inkjet-printed point-of-care immunoassay on a nanoscale polymer brush enables subpicomolar detection of analytes in blood. *Proc Natl Acad Sci U S A* **2017,** *114* (34), E7054-E7062.
2. Hucknall, A.; Kim, D.-H.; Rangarajan, S.; Hill, R. T.; Reichert, W. M.; Chilkoti, A., Simple Fabrication of Antibody Microarrays on Nonfouling Polymer Brushes with Femtomolar Sensitivity for Protein Analytes in Serum and Blood. *Advanced Materials* **2009,** *21* (19), 1968-1971.
3. Fontes, C. M.; Lipes, B. D.; Liu, J.; Agans, K. N.; Yan, A.; Shi, P.; Cruz, D. F.; Kelly, G.; Luginbuhl, K. M.; Joh, D. Y.; Foster, S. L.; Heggestad, J.; Hucknall, A.; Mikkelsen, M. H.; Pieper, C. F.; Horstmeyer, R. W.; Geisbert, T. W.; Gunn, M. D.; Chilkoti, A., Ultrasensitive point-of-care immunoassay for secreted glycoprotein detects Ebola infection earlier than PCR. *Sci Transl Med* **2021,** *13* (588).
4. McKenna, A.; Hanna, M.; Banks, E.; Sivachenko, A.; Cibulskis, K.; Kernytsky, A.; Garimella, K.; Altshuler, D.; Gabriel, S.; Daly, M.; DePristo, M. A., The Genome Analysis Toolkit: a MapReduce framework for analyzing next-generation DNA sequencing data. *Genome Res* **2010,** *20* (9), 1297-303.
5. Li, H.; Durbin, R., Fast and accurate short read alignment with Burrows-Wheeler transform. *Bioinformatics* **2009,** *25* (14), 1754-60.
6. Danecek, P.; Bonfield, J. K.; Liddle, J.; Marshall, J.; Ohan, V.; Pollard, M. O.; Whitwham, A.; Keane, T.; McCarthy, S. A.; Davies, R. M.; Li, H., Twelve years of SAMtools and BCFtools. *Gigascience* **2021,** *10* (2).
7. O'Toole, Á.; Pybus, O. G.; Abram, M. E.; Kelly, E. J.; Rambaut, A., Pango lineage designation and assignment using SARS-CoV-2 spike gene nucleotide sequences. *BMC Genomics* **2022,** *23* (1), 121.
8. Heggestad, J. T.; Kinnamon, D. S.; Olson, L. B.; Liu, J.; Kelly, G.; Wall, S. A.; Oshabaheebwa, S.; Quinn, Z.; Fontes, C. M.; Joh, D. Y.; Hucknall, A. M.; Pieper, C.; Anderson, J. G.; Naqvi, I. A.; Chen, L.; Que, L. G.; Oguin, T., 3rd; Nair, S. K.; Sullenger, B. A.; Woods, C. W.; Burke, T. W.; Sempowski, G. D.; Kraft, B. D.; Chilkoti, A., Multiplexed, quantitative serological profiling of COVID-19 from blood by a point-of-care test. *Sci Adv* **2021,** *7* (26).